

Sarah K. Allawi  
Mohammed A. Akraa

Department of Physics,  
College of Education for  
Pure Sciences,  
University of Babylon,  
P.O. Box 4,  
Al-Hilla 51002,  
Babil, IRAQ



# Synthesis and Structural Characteristics of Natural Antibacterial Metal-Organic Complexes

Numerous chemical composites have been proposed to attack microorganisms. This study describes an environmentally friendly complex that is facilitated, accessible, and efficient. The residue that is left behind after applying Beetroot juice to aqueous metal solutions containing  $\text{CuSO}_4 \cdot 5\text{H}_2\text{O}$  and  $\text{AgNO}_3$  using the co-precipitation process is the product. The structural characteristics were examined using energy dispersive X-ray spectroscopy (EDX), field emission scanning electron microscopy (FE-SEM), and X-ray diffraction (XRD). The product's chemical composition includes organic components of sulfur, oxygen, and nitrogen, as well as metallic copper and/or silver. The results showed a nanocomposite with an average crystallite size of 9.14 nm and impurity-free spherical particles. Antibacterial activity was assessed using the conventional zone of inhibition (ZOI) test. The synthesized compound demonstrated good antibacterial activity against *S. Aureus* and *E. Coli*, with inhibition proportional to silver ion weight percent.

**Keywords:** Antibacterial agents; Chemical synthesis methods; Electron microscopy  
**Received:** 31 August 2024; **Revised:** 03 October; **Accepted:** 10 October 2024

## 1. Introduction

Bacteria, minuscule single-celled organisms, have had a tremendous impact on human history, often with fatal consequences. From ancient plagues to current pandemics, they have fueled medical and public health advances. Bacterial infections, such as the Black Death in the 14<sup>th</sup> century, have wiped out whole communities [1]. These epidemics produced significant social and economic turmoil. Bacteria have been associated with illnesses such as TB, cholera, typhoid fever, and bubonic plague, which are commonly transmitted by polluted water, food, or vectors such as fleas and mosquitos [2]. These illnesses have plagued humans for generations. Beyond sickness, microorganisms have flourished in filthy settings throughout wars, exacerbating the human cost of war [3-5].

Antibiotic abuse has resulted in antibiotic-resistant microorganisms, which pose a challenge to contemporary medicine. Diseases that were formerly manageable, such as MRSA and MDR-TB, are now threatening public health advances [6]. Numerous microbes are beneficial to the environment, digestion, and the production of food and medication. Advances in microbiology and public health have reduced bacterial illness consequences, underscoring the need for ongoing attention and innovation [7].

Antibacterial research has focused a lot of interest on metal-organic complexes due to their potential therapeutic applications and variety of forms. These complexes' antibacterial qualities can be strengthened while maintaining their biocompatibility and environmental friendliness by adding natural substances. In order to combat the growing issue of antibiotic resistance, this synthesis approach has potential for producing novel antibacterial drugs [8].

The synthesis of metal-organic complexes involves coordinating metal ions with organic ligands to create intricate structures with specific properties [9]. Natural compounds, like plant extracts, are rich sources of biologically active molecules that can act as effective ligands in these complexes [10]. By leveraging the combined effects of metal ions and natural ligands, researchers hope to develop powerful antibacterial agents with improved effectiveness and reduced toxicity [11]. Many studies have shown that metal-organic complexes created using natural compounds can fight bacteria. For example, Patel et al. developed a copper (II) complex with quercetin, a flavonoid in many fruits and vegetables. Numerous bacteria, including strains resistant to multiple drugs, were efficiently eliminated by this complex, regardless of whether they were Gram-positive or Gram-negative [12].

Möhler et al. studied the improvement of antibiotic commotion by creating metal-antibiotic complexes. They found that the complexes showed increased activity against  $\beta$ -lactamase-producing bacteria, especially those formed with Ag(I) [13].

Drug release from zirconium metal-organic Framework (MOF) in reaction to pH variations and interactions with biomimetic schemes was studied by El-Bindary et al. The study showed the capacity to destroy cancer cells and release drugs in response to pH. According to the research, DOX@Zr-MOF appears to be a potentially effective method of delivering medications to cancer cells. Additionally, the antibacterial activity of DOX@Zr-MOF against *Escherichia coli* was assessed and found to be encouraging [14].

This work aims to explore the synthesis of antibacterial metal-organic complexes that incorporate natural compounds. We will discuss different strategies for designing these complexes, including the selection of metal ions and natural ligands, as well as the characterization of their antibacterial activity.

## 2. Materials and Method

A metal-organic complex was created by combining particular amounts of silver nitrate ( $\text{AgNO}_3$ ) and pentahydrate copper sulfate ( $\text{CuSO}_4 \cdot 5\text{H}_2\text{O}$ ) in a prescribed beaker. The mixture was then dissolved in deionized water, paying close attention to ensure thorough dissolution and stirring with a glass rod for approximately five minutes. Following that, a specific percentage of beetroot juice was added using the principles outlined in table (1).

**Table (1) The weight percent for the metal- organic complex with Beet juice**

Sample	$\text{AgNO}_3$ (gm)	$\text{CuSO}_4$ (gm)	Deionized Water (mL)	Beetroot juice (mL)
S <sub>1</sub>	0	5	200	50
S <sub>2</sub>	1	4	200	50
S <sub>3</sub>	2	3	200	50
S <sub>4</sub>	3	2	200	50
S <sub>5</sub>	4	1	200	50
S <sub>6</sub>	5	0	200	50

The beakers were covered with aluminum foil and allowed to settle at room temperature for two days. Further, the sediments were removed from the supernatant by a centrifuge. The precipitates were then dehydrated in Petri plates at room temperature.

Various analytical approaches were used to characterize the nanostructure products. The metal-organic complex's structural characteristics were studied using a Bruker D8 X-ray diffractometer (XRD) from Germany. The XRD was fitted with an ambient and temperature control stage, and operated with  $\text{Cu K}\alpha 1$  radiation ( $\lambda = 1.5406 \text{ \AA}$ ) at 40 kV and 100 mA. In addition, the Hitachi variable-pressure field-emission scanning electron microscope (FE-SEM) was used.

The antibacterial activity of the synthesized nanocomposites was evaluated using the agar disc diffusion method. In this process, Petri dishes containing 20 mL of Mueller Hinton agar were sterilized. Subsequently, 6 mm diameter discs from each prepared solvent were inserted into each Petri dish after the media solidified for five minutes. Next, 0.1 mL of every bacterial isolate was applied to the surface of the medium. After that, the Petri plates were kept in an incubator for 24 hours at  $37^\circ\text{C}$ . The zones of inhibition were measured and reported in millimeters, and the experiment was carried out in triplicate.

## 3. Results and Discussion

The structural properties of the metal-organic complexes were analyzed using XRD. In Fig. (1), the

XRD patterns for the metal-organic complexes at various concentrations are presented. It is evident from the figure that samples S<sub>1</sub>, S<sub>2</sub>, S<sub>3</sub>, and S<sub>4</sub> exhibit semi-amorphous characteristics with weak diffraction peaks. On the other hand, an increase in the concentration of  $\text{AgNO}_3$  in samples S<sub>5</sub> and S<sub>6</sub> resulted in a noticeable enhancement in crystallinity, as evidenced by distinct diffraction peaks observed at  $28.109^\circ$ ,  $31.849^\circ$ ,  $37.775^\circ$ ,  $46.141^\circ$ ,  $54.795^\circ$ ,  $57.123^\circ$ , and  $76.697^\circ$ . These angles correspond to the Miller indices of the reflecting planes (210), (112), (111), (231), (142), (241), and (311) planes of crystallites, which are attributed to the silver-organic nanoparticles (Ag NPs) based on the face-centered cubic structure (JCPDS card no. 04-0783) [15,16]. The crystallite size  $D$  was calculated using the Debye-Scherrer equation:

$$D = \frac{0.9\lambda}{\beta \cos \theta} \quad (1)$$

where  $\theta$  is the Bragg's angle,  $\beta$  is the full-width at half maximum (FWHM) of the diffraction peak, and  $\lambda$  is the radiation wavelength. The composites' average crystallite size was 9.14 nm. Table (2) provides a summary of the attributes that were inferred from the XRD investigation.

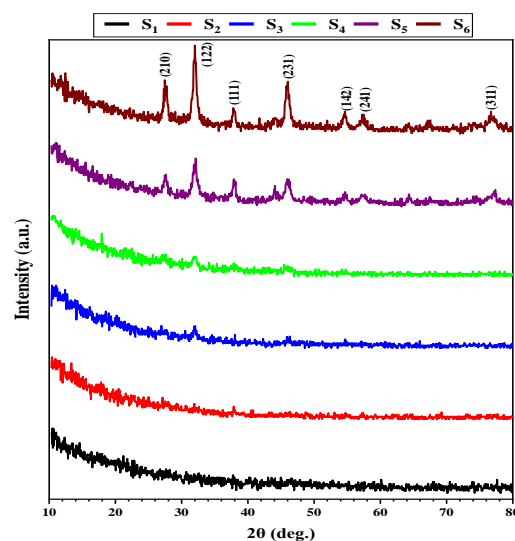


**Fig. (1) XRD spectra for the different concentrations of  $\text{AgNO}_3/\text{CuSO}_4$  composites with Beet juice**

This study used FE-SEM to examine the morphological properties of the metal-organic complexes. The FE-SEM pictures in Fig. (2) show how the nanoparticles are shaped by the silver ions. All the compounds showed spherical nanoparticle shape, with the exception of the first silver ion-free sample, which has a homogeneous distribution of nanoparticles. This shows that these composites, which have an average particle size of 30 nm, were successfully fabricated. These particle sizes are notably greater than the typical crystallite sizes (of 9.14 nm) found by XRD, indicating the aggregation of many crystallites [15].

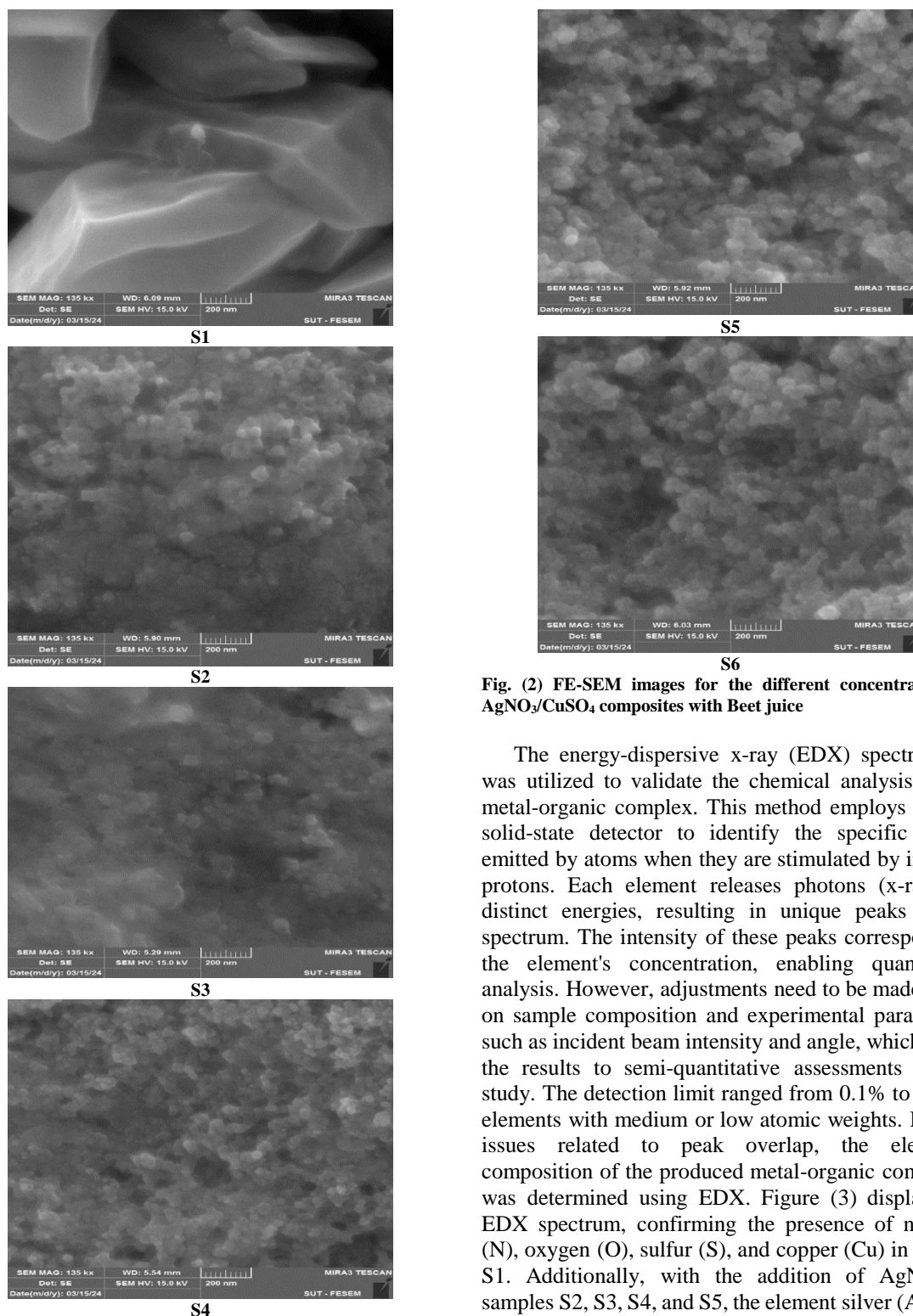
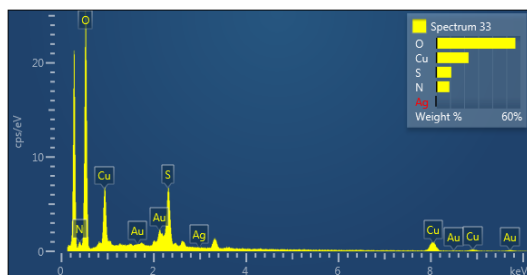


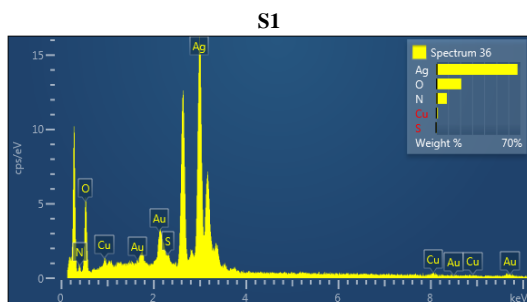
**Fig. (2) FE-SEM images for the different concentrations of  $\text{AgNO}_3/\text{CuSO}_4$  composites with Beet juice**

The energy-dispersive x-ray (EDX) spectroscopy was utilized to validate the chemical analysis of the metal-organic complex. This method employs a Si-Li solid-state detector to identify the specific x-rays emitted by atoms when they are stimulated by incident protons. Each element releases photons (x-rays) at distinct energies, resulting in unique peaks in the spectrum. The intensity of these peaks corresponds to the element's concentration, enabling quantitative analysis. However, adjustments need to be made based on sample composition and experimental parameters, such as incident beam intensity and angle, which limits the results to semi-quantitative assessments in this study. The detection limit ranged from 0.1% to 1% for elements with medium or low atomic weights. Despite issues related to peak overlap, the elemental composition of the produced metal-organic complexes was determined using EDX. Figure (3) displays the EDX spectrum, confirming the presence of nitrogen (N), oxygen (O), sulfur (S), and copper (Cu) in sample S1. Additionally, with the addition of  $\text{AgNO}_3$  in samples S2, S3, S4, and S5, the element silver (Ag) was detected alongside other elements (N, O, S, Cu) in varying concentrations. However, in sample S6, copper was no longer present, and silver accounted for a higher percentage (36.85%), consistent with the experimental findings. The uniform distribution of these elements was confirmed through elemental mapping using the FE-SEM. This mapping demonstrates the well-dispersed nature of nitrogen, oxygen, sulfur, copper,

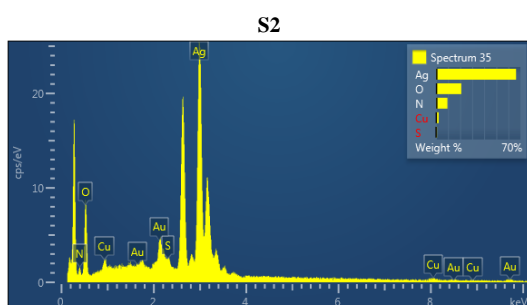
and silver throughout the composite. Overall, our data strongly endorse the homogeneity and high purity of the produced metal-organic complex [15].



Element	Atomic %
N	13.80
O	71.87
S	6.91
Cu	7.43
<b>Total:</b>	<b>100</b>

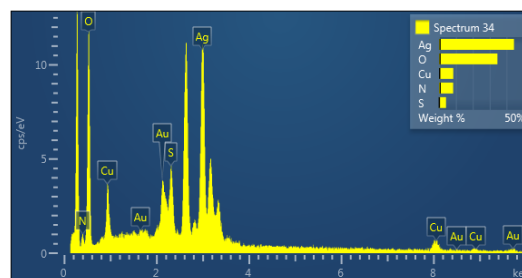


Element	Atomic %
N	17.40
O	62.96
S	3.76
Cu	3.89
Ag	11.99
<b>Total:</b>	<b>100</b>

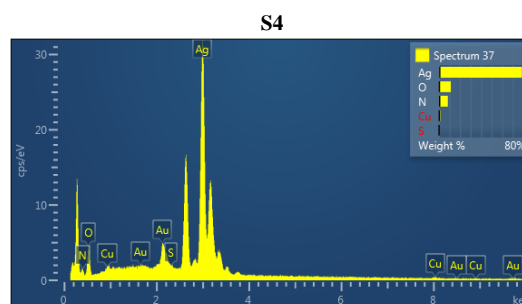


Element	Atomic %
N	24.48
O	49.84
S	0.90
Cu	0.97
Ag	23.82
<b>Total:</b>	<b>100</b>

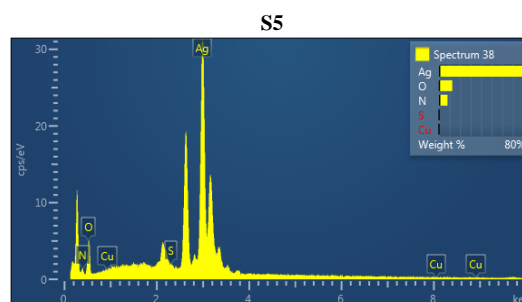
S3



Element	Atomic %
N	25.53
O	49.11
S	0.96
Cu	1.34
Ag	23.07
<b>Total:</b>	<b>100</b>



Element	Atomic %
N	29.02
O	33.86
S	0.66
Cu	0.98
Ag	35.49
<b>Total:</b>	<b>100</b>



Element	Atomic %
N	27.23
O	37.46
S	0.46
Ag	36.85
<b>Total:</b>	<b>100</b>

S6

Fig. (3) EDX results for the different chemical composition of the precipitated metal-organic complex

The antibacterial efficacy of the precipitated metal-organic complex samples was assessed using the agar well diffusion assay against Gram-positive and Gram-negative bacterial strains [17]. Inoculate bacterial



species from stock cultures using a sterile wire loop into Petri dishes containing 20 mL of Muller-Hinton (MH) agar [18]. After culturing the organisms, we used a sterile tool to create 6 mm-diameter wells on the agar plates. Following this, we introduced various chemical compositions of the metal-organ complex samples into the bored wells. The plates, with the composite samples and test organisms, were then incubated at 37°C overnight. Subsequently, the average diameter of the zones of inhibition was measured and recorded.

All results of the antibacterial activity with different concentrations are shown in figures (4) and (5) below all details explained in table (3). With increasing the silver ion concentration in the chemical composition of the metal-organic complex, the inhibition zones increased, which increased from 17 mm to 27 mm for *E. coli* and from 18 mm to 26 mm for *S. aureus* at a concentration of 1000 µg/mL.

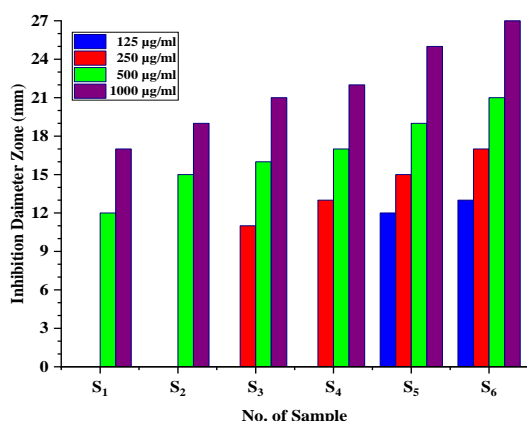


Fig. (4) Antibacterial activity of the metal-organic complex against *E. coli* with different concentrations (125, 250, 500 and 1000 µg/mL)

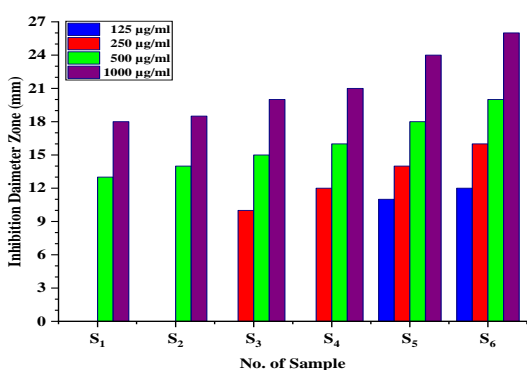


Fig. (5) Antibacterial activity of the metal-organic complex against *S. aureus* with different concentrations (125, 250, 500 and 1000 µg/mL)

Table (3) The antibacterial activity of nanoparticles

Antibacterial analysis (Zone of inhibition (mm))						
Sample	S <sub>1</sub>	S <sub>2</sub>	S <sub>3</sub>	S <sub>4</sub>	S <sub>5</sub>	S <sub>6</sub>
<i>E. coli</i>	17	19	21	22	24	27
<i>S. aureus</i>	18	19	21	24	25	26

#### 4. Conclusions

The metal-organic complex powder was successfully synthesized using a co-precipitation process. The average crystallite size was determined to be 9.14 nm and spherical morphology for the produced precipitate was confirmed with homogenous and uniform distribution. The product as a metal-organic compound was free from impurities. The synthesized nanocomposites demonstrated significant antibacterial activity against *E. coli* and *S. aureus* bacteria in a dose-dependent manner.

#### References

- [1] M. Neill, H. William, "Plagues and Peoples", 1<sup>st</sup> ed., Anchor Books (2015), Ch. 3, p. 220.
- [2] M. Morens et al., "The Challenge of Emerging and Re-Emerging Infectious Diseases", *Nature*, 430(6996) (2004) 242-24.
- [3] T.J. Gerard, F.R. Berdell and C.L. Christine, "Microbiology: An Introduction", 13<sup>th</sup> ed., Pearson (2015), Ch. 5, p. 480.
- [4] S. Sethi, S. Das and M. Dash, "Rendezvous with the pandemic survivors: An analysis of the Spanish flu in Katherine Anne Porter's 'Pale horse, pale rider' and COVID-19", *Rupkatha J. Interdiscip. Stud. Human.*, 12(5) (2020) 1-7.
- [5] D. Julian, "Origins and Evolution of Antibiotic Resistance", *Microbiol. Mol. Biol. Rev.*, 74(3) (2010) 417-433.
- [6] K. Marianna and T. Gregory, "Infectious Diseases in Ancient Times: An Overview", *Infect. Drug Resist.*, 12 (2019) 2377-2382.
- [7] G. Martin, "Trench Fever in the First World War", *The Lancet Infect. Dis.*, 16(3) (2016) 298-299.
- [8] Y. Si et al., "An efficient metal-organic framework-based drug delivery platform for synergistic antibacterial activity and osteogenesis", *J. Colloid Interface Sci.*, 640 (2023) 521-539.
- [9] A.A.R. Mahmood et al., "Some Physical Properties of Metal-Hydroxyquinoline Complexes in Different Solvents", *Iraqi J. Appl. Phys.*, 17(1) (2021) 9-16.
- [10] A.A. Mahmood et al., "Preparation and Photoluminescence Spectra of Organometallic Complexes Containing Nanoparticles as Random Gain Media", *Indonesian J. Chem.*, 22(1) (2022) 205-211.
- [11] Z. Chen et al., "Metal-organic framework-based advanced therapeutic tools for antimicrobial applications", *Acta Biomaterialia*, 175 (2023) 27-54.
- [12] M.N. Patel et al., "Synthesis, characterization and antibacterial activity of copper (II) complex of quercetin", *J. Mol. Struct.*, 1(185) (2019) 526-531.
- [13] J.S. Möhler et al., "Enhancement of antibiotic-activity through complexation with metal ions-Combined ITC, NMR, enzymatic and biological studies", *J. Inorg. Biochem.*, 167 (2017) 134-141.

- [14] M.A. El-Bindary, M.G. El-Desouky and A.A. El-Bindary, "Metal-organic frameworks encapsulated with an anticancer compound as drug delivery system: Synthesis, characterization, antioxidant, anticancer, antibacterial, and molecular docking investigation", *Appl. Organomet. Chem.*, 36(5) (2022) 1-16.
- [15] Y. Meng, "A sustainable approach to fabricating Ag nanoparticles/PVA hybrid nanofiber and its catalytic activity", *Nanomater.*, 5(2) (2015) 1124-1135.
- [16] R.I. Priyadharshini et al., "Microwave-mediated extracellular synthesis of metallic silver and zinc oxide nanoparticles using macro-algae (*Gracilaria edulis*) extracts and its anticancer activity against human PC3 cell lines", *Appl. Biochem. Biotechnol.*, 174 (2014) 2777-2790.
- [17] L. Nie et al., "Silver-doped biphasic calcium phosphate/alginate microclusters with antibacterial property and controlled doxorubicin delivery", *J. Appl. Polym. Sci.*, 138(19) (2020) 1-13.
- [18] H.M. Yusof et al., "Antibacterial potential of biosynthesized zinc oxide nanoparticles against poultry-associated foodborne pathogens: an in vitro study", *Animals*, 11(7) (2021) 2093.

Table (2) The XRD parameters for the metal-organic complexes with Beetroot juice

2 Theta (deg)	Phase ID	(hkl)	d spacing (nm)	FWHM (deg)	Crystallite size (nm)	Average Crystallite Size (nm)
28.109	Ag	(210)	3.23916	0.620	13.80	9.14
31.849	Ag	(122)	2.79897	0.787	10.97	
37.775	Ag	(111)	2.37549	1.574	5.57	
46.141	Ag	(231)	1.97090	1.180	7.65	
54.795	Ag	(142)	1.68110	0.900	10.39	
57.123	Ag	(241)	1.60581	1.100	8.59	
76.697	Ag	(311)	1.24107	1.500	7.06	